Supplementary Material 1: *Effect of extracellular water*

We compared the ability of our clinical qPFG diffusion MRI sequences to resolve human axons with different diameters in the presence of various amounts of extra-cellular signal. **Fig. S1** shows the theoretical angular qPFG diffusion attenuation curves for experiments with $\tau_m = 13.4\ ms$ (top row) and $\tau_m = 0\ ms$ (bottom row) assuming 100%, 70% and 40% intra-axonal signal. Diffusivities of $D = 1.5\ \mu m^2/ms$ and $D_0 = 0.7\ \mu m^2/ms$ were used for the intra-axonal and extracellular signal components.

Our results indicate that, despite the larger pulse width 2δ of the fused gradient pulse, the $\tau_m = 0\ ms$ sequence still results in a large positive angular modulation for axons with diameters between $1 - 10\ \mu m$. In fact, the amplitude of this positive modulation obtained for $\tau_m = 0\ ms$ is larger than that obtained with $\tau_m = 13.4\ ms$ and increases for larger axon diameters up to $8\ \mu m$. When the contribution of extracellular water is added, the profile amplitude for $\tau_m = 0\ ms$ becomes negative for small axons. For axons with larger diameters and small intra-axonal signal fractions of 40% the profiles can exhibit multiple local extrema, similar to those generated by fiber misalignment. In these cases it is crucial to use accurate fiber orientation estimates in the extraction of microscopic anisotropy parameters. Overall, extracellular water decreases the ability to resolve axons with different diameters in measurements with $\tau_m = 0\ ms$ and $\tau_m = 13.4\ ms$ alike. When datasets with zero and non-zero values of τ_m are fit simultaneously, the confounding signals from unrestricted extracellular water are qualitatively different (Fig. 5) and can be disentangled more efficiently.

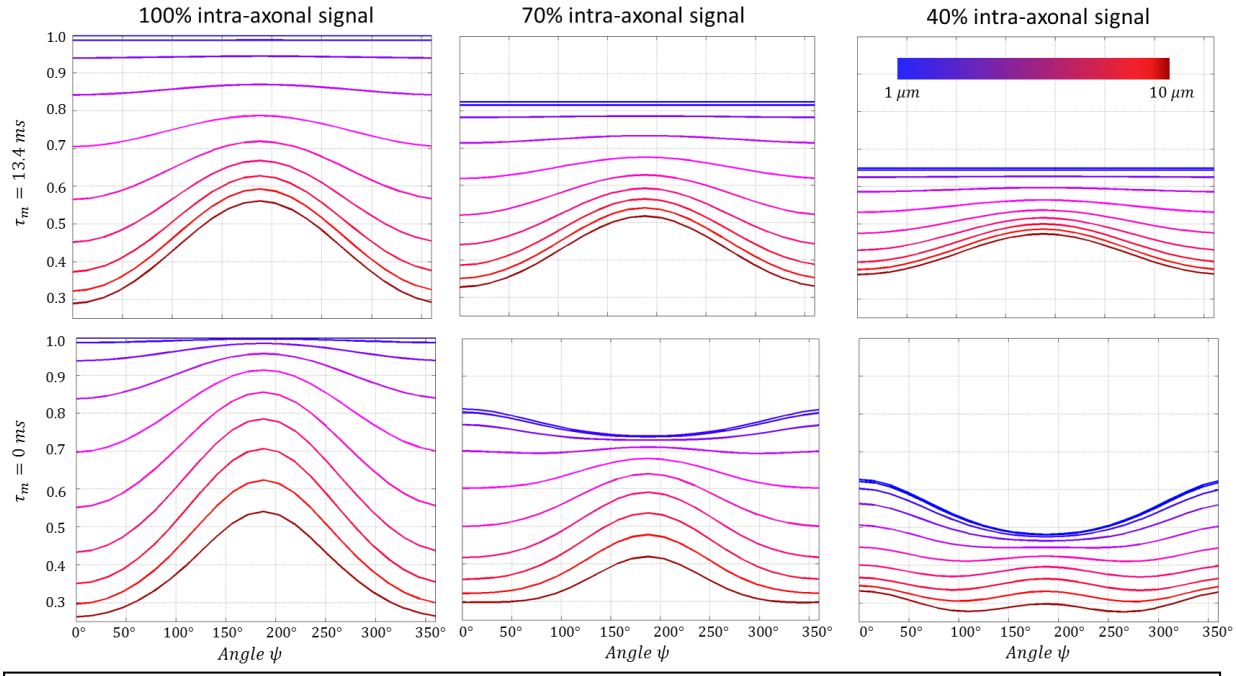

Figure S1: Comparison of sensitivity to axon diameter for the proposed clinical qPFG MRI sequence designs with $\tau_m = 13.4\ ms$ (top row) and $\tau_m = 0\ ms$ (bottom row) assuming 100%, 70% and 40% intra-axonal signal fractions and qPFG diffusion encoding applied orthogonal to the fiber orientation. $D = 1.5\ \mu m^2/ms$ and $D_0 = 0.7\ \mu m^2/ms$ were used for the diffusivities in the intra-axonal and extracellular signal components.

Supplementary Material 2: *Robustness of qPFG methodology*

A healthy human volunteer was scanned using the same protocol detailed in the manuscript but with qPFG diffusion encoding applied in three separate planes (xy, yz and zx, as shown in **Fig. S2**) to probe extreme scenarios of orientation mismatch with respect to the underlying microanatomy. For each plane 4 averages with both $\tau_m = 13.4\,ms$ and $\tau_m = 0\,ms$ were acquired using 12 angles to sample the entire $0° - 360°$ range. To investigate the ability of the three qPFG diffusion encoding schemes to discriminate axons with different diameters we simulated the angular profiles for the case when $\tau_m = 13.4\,ms$ using an intra-axonal diffusivity of $D = 1.5\,\mu m^2/ms$. Subsequently, we fit our tissue model (using the same high-resolution DTI information) to individual datasets. In addition, a combined dataset containing all 36 qPFG MRI measurements was generated (column 4 in **Fig. S2**) and processed similarly to serve as control.

As expected, the ability of qPFG MRI to resolve axons of different diameters varies sensitively with fiber orientation. The sensitivity to restriction-induced microscopic anisotropy is maximized when both $\boldsymbol{q_1}$ and $\boldsymbol{q_2}$ are applied orthogonal to the fiber orientation. With qPFG diffusion encoding applied in different planes, coupling with macroscopic anisotropy reduces both the sensitivity to axon diameters and the overall signal-to-noise ratio due to increased diffusion attenuation of intra-axonal water along the axial direction. This effect is maximized when $\boldsymbol{q_1}$ is applied axially, as shown for the zx plane dataset, resulting in non-physical values for estimated model parameters. On the other hand, measurements acquired with qPFG encoding in the $xy-$ and $yz-$planes resulted in similar maps of average axon diameters d and intra-axonal signal fractions f. Moreover, these maps are comparable to those obtained by fitting the model to the large control dataset containing all qPFG diffusion measurements. These preliminary results confirm the robustness of our methodology in the presence of sufficient SNR and its potential for full-brain applications. Differences between microscopic anisotropy parameter maps estimated with different qPFG diffusion encoding schemes could be caused by intra-voxel fiber orientation and diameter distributions, subject motion during the long scan duration and inconsistent SNR and axon diameter sensitivity.

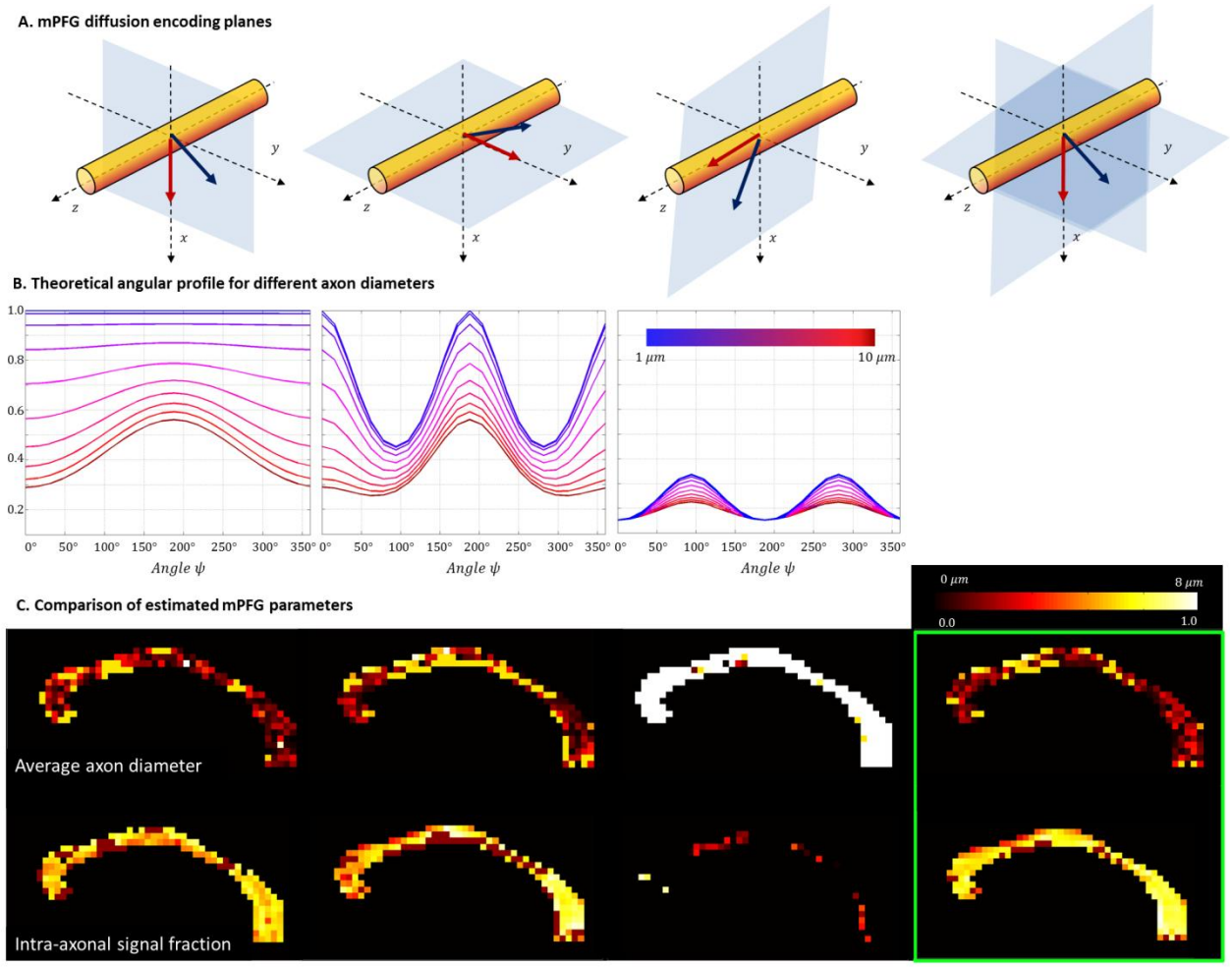

Figure S2: A. Application of diffusion encoding blocks $\boldsymbol{q_1}$ (red) and $\boldsymbol{q_1}$ (black) for encoding in the xy-, yz- and zx-planes corresponding to columns 1-3 respectively. To serve as control, an additional dataset was generated by combining the measurements in all 3 datasets (column 4). **B.** Theoretical ψ-dependence of diffusion signal attenuation for qPFG experiments with $\tau_m = 13.4\ ms$ and corresponding diffusion encoding schemes shown above, assuming intra-axonal diffusivity of $D = 1.5\ \mu m^2/ms$. **C.** Microscopic anisotropy parameters estimated from individual datasets result in similar distributions, provided sufficient signal-to-noise ratio.